4030 *Chem. Mater.* **2009,** *21,* 4030–4036
DOI:10.1021/cm901383x

CHEMISTRY OF MATERIALS
Article

Pd−C−Fe Nanoparticles Investigated by X-ray Absorption Spectroscopy as Electrocatalysts for Oxygen Reduction

Yun-Chieh Yeh,[†] Hao Ming Chen,[†] Ru-Shi Liu,*[,†] Kiyotaka Asakura,[‡] Man-Yin Lo,[§] Yu-Min Peng,[§] Ting-Shan Chan,[&] and Jyh-Fu Lee[&]

[†]*Department of Chemistry, National Taiwan University, Taipei 106, Taiwan, Republic of China,* [‡]*Catalysis Research Center, Hokkaido University, Hokkaido 001-0021, Japan,* [§]*Material and Chemical Research Laboratories, Industrial Technology Research Institute, Hsinchu 300, Taiwan, Republic of China, and* [&]*National Synchrotron Radiation Research Center, Hsinchu 300, Taiwan, Republic of China*

Received May 20, 2009. Revised Manuscript Received July 3, 2009

Carbon-supported PdCFe/C catalyst was synthesized by impregnation method. X-ray absorption spectroscopy (XAS) revealed the incorporation of C atoms in PdFe/C clusters and high-temperature annealing was facilitated the formation of the Pd−Fe−C alloy. The catalytic activity oxygen operated via reduction reaction (ORR) of Pd−Fe−C alloy demonstrated the strong dependence upon composition of Pd−Fe−C catalysis, the half-wave potential raise with the increase of iron content. A cyclic voltammetry (CV) test conducted in methanol/ perchloric acid mixed solution was employed to elucidate the tolerance of PdCFe/C electrocatalysts for methanol, which exhibited the methanol-proof character of PdCFe/C electrocatalysts.

Introduction

Direct methanol fuel cells (DMFCs) have been regarded as potential next-generation power sources. Electrocatalysts have been extensively studied to promote catalytic activity. Platinum-based alloys[1−3] have been demonstrated to be effective electrocatalysts in DMFCs. However, disadvantages such as low tolerance toward methanol[4,5] and the high cost of platinum[6,7] restrict its application. Therefore, numerous nonplatinum catalysts, such as transition-metal oxides,[8] transition-metal macrocycles,[9] and palladium-based catalysts,[10−13] have been extensively investigated.

Palladium is less expensive than platinum, but it performs less efficiently in oxygen reduction reactions (ORRs). Recent investigations have proven that an alloy of palladium with other transition metals can increase the catalytic activity toward ORRs.[10−14] Shao et al.[11] showed that electrocatalysts formed by alloying palladium and iron in a 3:1 molar ratio (Pd_3Fe/C) exhibit the greatest activity toward ORRs, with a half-wave potential that is ∼20 mV greater than that of Pt/C from ETEK. However, PdFe/C, which has been used as an electrocatalyst elsewhere,[12,13] has a half-wave potential that is lower than that of Pt/C from ETEK. Most investigations on this subject take into account the change in catalytic activity that is associated with lattice distortion caused by the formation of the alloy.[15] The change in interatomic distance is believed to influence the adsorption and transfer of oxygen-containing species in ORRs.[11,18] Lattice distortion also influences the orbital overlap, altering the electronic properties[16−18] on the active site of the electrocatalyst. Changing the electronic properties affects the surface reactivity, altering the performance of the electrocatalyst.

Structure affects the intrinsic properties of an electrocatalyst. Therefore, structural analysis helps to elucidate the catalytic mechanism. Extended X-ray absorption fine structure (EXAFS) analysis is a powerful tool in obtaining structural information on noncrystalline and crystalline materials.[19−22] A structure with short-range order

*Author to whom correspondence should be addressed. Tel.: +886-2-3366-1169. Fax: +886-2-2363-6359. E-mail: rsliu@ntu.edu.tw.

(1) Mukerjee, S; Srinivasan, S.; Soriaga, M.; McBreen, J. *J. Electrochem. Soc.* **1995**, *142*, 1409.
(2) Stamenkovic, V.; Schmidt, T. J.; Ross, P. N.; Markovic, N. M. J. *J. Phys. Chem. B* **2002**, *106*, 11970.
(3) Toda, T.; Igarashi, H.; Uchida, H.; Watanabe, M. *J. Electrochem. Soc.* **1999**, *146*, 3750.
(4) Jarvi, T. D.; Stuve, S.; Sriramulu, E. M. *J. Electrochem. Soc.* **2000**, *147*, 4605.
(5) Schmidt, T. J.; Paulus, U. A.; Gasteiger, H. A.; Alonso-Vante; Behm, R. J. *J. Electrochem. Soc.* **2000**, *147*, 2620.
(6) Jiang, R. Z.; Chu, D. Y. *J. Phys. Chem. B* **1997**, *101*, 3646.
(7) Ralph, T. R.; Hogarth, M. P. *Platinum Met. Rev.* **2002**, *147*, 4605.
(8) Zen, J. M.; Wang, C. B. *J. Electrochem. Soc.* **1994**, *141*, L51.
(9) Zhong, H.; Zhang, H.; Liu, H.; Liang, Y. M.; Hu, J. W.; Yi, B. L. *Electrochem. Commun.* **2006**, *8*, 707.
(10) Fenandze, J. L.; Walsh, D. A.; Bard, A. J. *J. Am. Chem. Soc.* **2005**, *127*, 357.
(11) Shao, M. -H; Sasaki, K.; Adzic, R. R. *J. Am. Chem. Soc.* **2006**, *128*, 3526.
(12) Shao, M. -H; Liu, P.; Zhang, J. L.; Adzic, R. *J. Phys. Chem. B* **2007**, *111*, 6772.
(13) Wang, R.; Liao, S.; Fu, Z.; Ji, S. *Electrochem. Commun.* **2008**, *10*, 523.
(14) Savadogo, O.; Lee, K.; Oishi, K.; Mitsushima, S.; Kamiya, N.; Ta, K. I. *Electrochem. Commun.* **2004**, *6*, 105.
(15) Jalan, V.; Taylor, E. J. *J. Electrochem. Soc.* **1983**, *130*, 2299.
(16) Hwmmer, B.; Norskov, J. K. *Adv. Catal.* **2000**, *45*, 71.
(17) Min, M.-K.; Cho, J.; Cho, K.; Kim, H. *Electrochim. Acta* **2000**, *45*, 4211.
(18) Wang, X. Y.; Balbuena, P. B. *J. Phys. Chem. B* **2005**, *109*, 18902.
(19) Chen, H. M.; Liu, R.-S.; Asakura, K.; Lee, J.-F.; Jang, L.-Y.; Hu, S.-F. *J. Phys. Chem. B* **2006**, *110*, 19162.
(20) Chen, H. M.; Liu, R. S.; Jang, L.-Y.; Lee, J.-F.; Hu, S.-F. *Chem. Phys. Lett.* **2006**, *421*, 118.

 Published on Web 08/07/2009

can be probed using the EXAFS technique; in particular, the nearest-neighbor interatomic distances and coordination number can be determined. EXAFS is element-specific and can yield the local structure around a selected atom in samples that contain numerous metal atoms. In this study, the PdCFe/C electrocatalyst that is synthesized by an impregnation method was studied by X-ray absorption microscopy. A possible mechanism of formation of PdCFe/C electrocatalysts is proposed based on the structural parameter obtained from EXAFS.

Experimental Section

Chemicals and Materials. Ferrous nitrate (99%, Aldrich), methanol (99.8%, Aldrich), perchloric acid (70%, Acros Organics), and Pd/C (20 wt % loading, ETEK) were used without purification. The water used throughout the experiment was reagent-grade and was produced using a Milli-Q SP ultrapure-water purification system (Nihon Millipore, Ltd., Tokyo, Japan).

Synthesis of Carbon-Supported PdCFe Catalyst. An impregnation method was adopted to synthesize the PdCFe/C electrocatalyst. The Pd/C was initially mixed with the required amount of $Fe(NO_3)_3$ solution, sonicated until uniformly dispersed, and then dried at 80 °C in air. The obtained powder was finally calcined at 500 °C for 5 h under 5% H_2 (mixed with 95% nitrogen) and cooled to room temperature at a rate of 5 °C/min. For comparison, Pd/C (20 wt % loading) and Pt/C (40 wt % loading, obtained from ETEK) were treated under the same calcination conditions.

Electrode Preparation and Electrochemical Measurements. A module of three electrodes was used in an electrochemical test. A glassy carbon electrode (GC electrode, 5 mm in diameter, PINE: AFE3T050GC) was used as the working electrode; a platinum plate served as the counter electrode and a standard hydrogen electrode (SHE) was used as the reference electrode. A uniformly dispersed electrocatalyst slurry was obtained via an ultrasonic dispersal of electrocatalysts in deionized water. To prepare the electrode, the GC electrode was initially polished using 0.05 μm alumina powder, and then 15 μL of the electrocatalyst slurry was placed on the working electrode, which was dried in air at 40 °C. Finally, the catalyst-loaded GC electrode was covered with 20 μL of a 1% Nafion solution diluted using isopropyl alcohol and dried in a N_2 atmosphere. Cyclic voltammograms (CVs) were obtained in the N_2 atmosphere in 0.1 M perchloric acid electrolyte, at a scan rate of 10 mV/s with 20 cycles between 0 V and 1 V. The ORR was performed in an oxygen-saturated 0.1 M perchloric acid electrolyte with a rotating disk electrode (RDE) that rotated/revolved at 1600 rpm. All current−voltage ($I-V$) curve measurements were made using a potentiostat (Eco Chemie AUTOLAB (The Netherlands)) at 30 °C and GPES (General Purpose Electrochemical System) software.

X-ray Absorption Spectroscopy (XAS). The Pd and Fe K-edge XAS spectra were obtained in transmission mode at the BL01C1 beamline facility at the National Synchrotron Radiation Research Center (NSRRC). The BL01C1 beamline takes 2 mrad of radiation from the tip of the left wing of the horizontal radiation fan of the superconducting-wavelength-shifter (SWLS) X-ray source. The energy resolution ($\Delta E/E$) estimated from the rocking curves of the double-crystal Si (111) monochromator is $(1.7-3.0) \times 10^{-4}$ in the energy range of 6−33 keV. The ion chambers used to measure the incident beam intensity (I_0) and transmitted beam intensity (I_t) in Pd K-edge XAS were filled with argon gas and a mixture of argon and krypton gases, respectively. To perform the Fe K-edge XAS measurement, a mixture of nitrogen and helium gases was introduced to the ion chambers, which were thus used to measure the incident intensity (I_0). To measure the transmitted beam intensity (I_t), a mixture of argon and nitrogen gases was adopted. Energy calibration was conducted using the first inflection point of the Pd K-edge (24350 eV) and Fe K-edge (7112 eV) absorption spectra of palladium metal and iron metal foils, respectively.

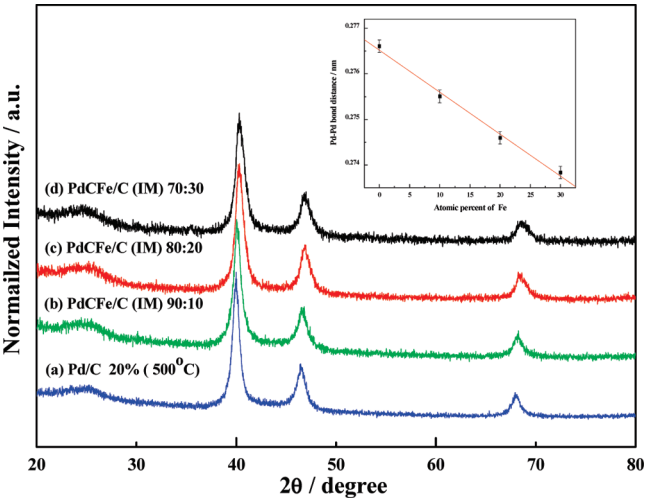

Figure 1. X-ray diffraction (XRD) diffraction patterns of (a) Pd/C 20% (500 °C), (b) PdCFe/C (IM) 90:10, (c) PdCFe/C (IM) 80:20, and (d) PdCFe/C (IM) 90:10 alloys obtained using Cu Kα (λ = 1.5418 Å) radiation. All samples were treated at 500 °C under a reductive atmosphere. Inset: Pd−Pd bond distance, calculated from XRD data, against concentration of Fe in PdCFe/C electrocatalysts.

EXAFS Analysis. EXAFS analyses were conducted using an analytical package called "REX2000", coded by Rigaku. Pre-edge and post-edge backgrounds were subtracted from the XAS spectra, and the results were normalized with respect to edge height. The extracted k^3-weighted EXAFS Pd K-edge and Fe K-edge spectra, $k^3x(k)$, were Fourier-transformed in the k-range of 3.0−15 Å^{-1} and 3.0−11.85 Å^{-1}, respectively. The Fourier-transformed peak was reverse Fourier-transformed by applying a Hanning window function. The filtered EXAFS data were analyzed by nonlinear least-squares curve fitting.[23] The back-scattered amplitude and phase shift functions for specific atom pairs were calculated using an FEFF7 code. The amplitude reduction factor (S_0^2) values for palladium and iron were fixed at 0.84 and 0.88, respectively, to determine the structural parameters for each bond pairs.

Results and Discussion

Figure 1 shows the XRD patterns of PdCFe/C catalysts. The diffraction peaks centered at 40°, 47°, and 68° correspond to the (111), (200), and (220) reflections, respectively, and a broad peak centered at ∼25°

(21) Chen, H. M.; Peng, H. M; Liu, R. S.; Hu, S. F.; Jang, L. Y. *Chem. Phys. Lett*. **2006**, *420*, 484.
(22) Bian, C.-R.; Suzuki, S.; Asakura, K.; Lu, P.; Toshima, N. *J. Phys. Chem. B* **2002**, *106*, 8587.
(23) Iwasawa, Y. *X-ray Absorption Fine Structure for Catalyst and Surfaces*; World Scientific: Singapore, 1996.

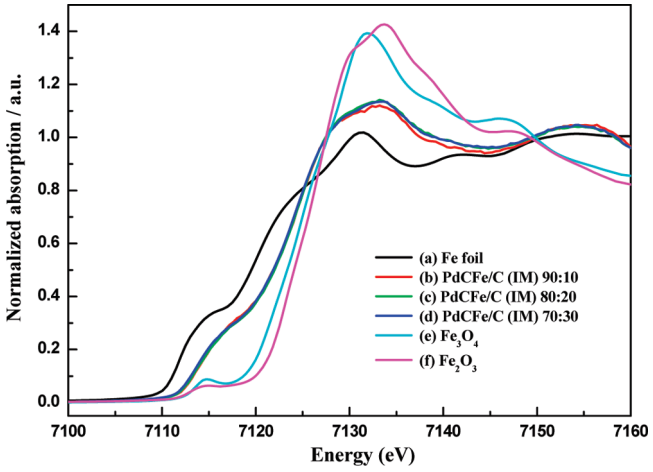

Figure 2. Fe K-edge XANES spectra of (a) iron foil, (b) PdCFe/C (IM) 90:10, (c) PdCFe/C (IM) 80:20, (d) PdCFe/C (IM) 70:30, (e) Fe_3O_4, and (f) Fe_2O_3.

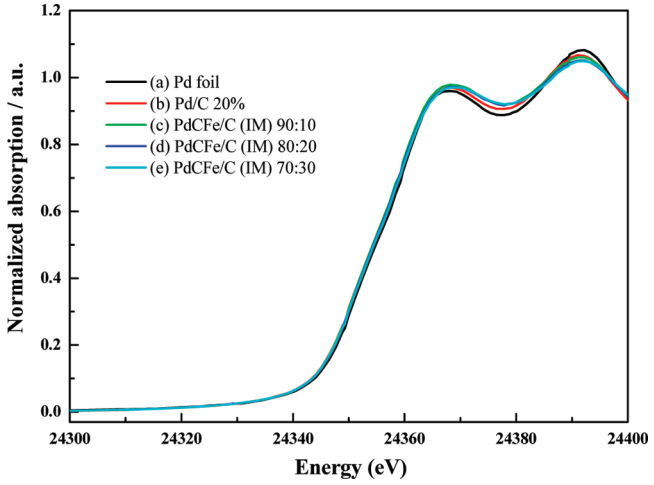

Figure 3. Pd K-edge XANES spectra of (a) palladium foil, (b) Pd/C 20% (500 °C), (c) PdCFe/C (IM) 90:10, (d) PdCFe/C (IM) 80:20, and (e) PdCFe/C (IM) 70:30.

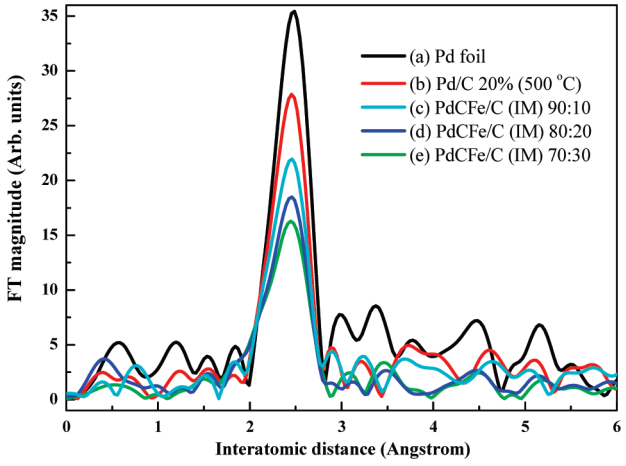

Figure 4. Pd K-edge FT-EXAFS spectra of (a) palladium foil, (b) Pd/C 20% (500 °C), (c) PdCFe/C (IM) 90:10, (d) PdCFe/C (IM) 80:20, and (e) PdCFe/C (IM) 70:30.

corresponds to the (002) plane reflection of an hexagonal structure in XC-72R. No peak characteristic of iron or iron oxides was observed in the diffraction pattern, suggesting the incorporation of Fe in an fcc lattice of Pd to form a single-phase solid solution, or the presence of highly dispersed Fe species. The inset plot exhibits the variation of Pd−Pd bond length, calculated from XRD data, as a function of the concentration of Fe in PdCFe/C electrocatalysts. The Pd−Pd bond length decreased as the iron content increased, revealing that different amounts of iron replaced palladium in the Pd lattice, which was thus differently distorted. Because the atomic radius of iron (1.27 Å) is less than that of palladium (1.38 Å), as shown in the inset in Figure 1, the Pd−Pd bond length decreased as the iron content increased. The variation in Pd−Pd bond length is caused by the variation in the amount of replacement iron in the Pd lattice.

X-ray absorption near edge structure (XANES) analysis is associated with the excitation of a core electron to bound and quasi-bound states. The edge position is related to the valence of the central atom.[23] Figure 2 presents the Fe K-edge XANES spectra of iron foil and PdCFe/C that was prepared via the impregnation method. The absorption edges of PdCFe/C electrocatalysts shifted to a higher energy than those of the iron foil, and the energy shift of the absorption edges in the PdCFe/C electrocatalyst is less than that of iron oxide species, such as Fe_2O_3 and Fe_3O_4; to this regard, the oxidation state of Fe in PdCFe/C electrocatalyst should be between that of metallic iron and iron oxide (i.e., formation of iron species with a lower oxidation state than that of iron oxide species in the PdCFe/C electrocatalysts). This small edge shift suggests that the atoms that surround the Fe atom should have a lower electronegativity than the O atom. The white line peak centered at 7130 eV, which corresponds to the transition from 1s to 4p in metallic iron, is partly enhanced in the case of PdCFe/C electrocatalysts compared with Fe foil, but is still lower than that of iron oxide species. Herein, iron carbide, as will be shown below in the EXAFS fitting results, is probably formed in PdCFe/C electrocatalysts.

Figure 3 presents the Pd K-edge XANES spectra of the PdCFe/C electrocatalysts. As shown in Figure 3, all of the PdCFe/C samples yield almost the same near-edge absorption structures as palladium foil, indicating the metallic character of palladium in all of the samples. Because heat treatment was performed in an H_2 (5%)/N_2 atmosphere, palladium oxide species may be reduced to the metallic state during annealing.

Based on the study of Sayers et al.,[26] EXAFS was Fourier-transformed, using the photoelectron wave vector, to yield information on nearest-neighbor coordination shells. Figure 4 shows the Fourier transforms of Pd K-edge spectra of PdCFe/C electrocatalysts and palladium foil. The main peak centered at ca. 2.6 Å is

(24) Schulman, R. G.; Yafet, Y.; Eisenberger, P.; Blumberg, W. E. *Proc. Natl. Acad. Sci. U.S.A.* **1976**, *73*, 1384.
(25) Roe, A. L.; Schneider, D. J.; Mayer, R. J.; Pyrz, J. W.; Widom, J.; Que, L. *J. Am. Chem. Soc.* **1984**, *106*, 1676.
(26) Sayers, D. E.; Stern, E. A.; Lytle, F. W. *Phys. Rev. Lett.* **1971**, *27*, 1204.

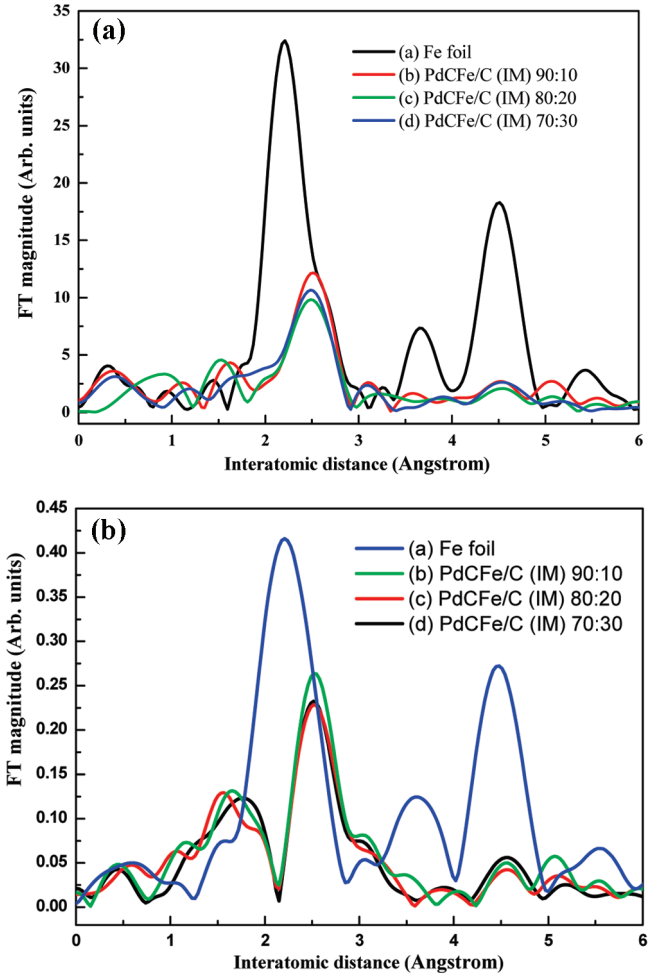

Figure 5. Fourier transforms of (a) k^3-weighted EXAFS oscillations and (b) k^1-weighted EXAFS oscillations for Fe K-edge FT-EXAFS spectra. (Legend: iron foil (spectrum a), PdCFe/C (IM) 90:10 (spectrum b), PdCFe/C (IM) 80:20 (spectrum c), and (d) PdCFe/C (IM) 70:30 (spectrum d).)

corresponds to Pd−Pd and Pd−Fe coordination in the first coordination shell. The intensity of the main peak declines as the amount of added iron increases. Therefore, the drop in the height of the Fourier-transformed peak revealed destructive interference between Pd−Pd and Pd−Fe oscillations caused by the formation of FePd alloy. Notably, the Pd−Pd bond distance did not vary with the PdFe content. This phenomenon is frequently observed in the bimetallic system in which the bond distances derived by XRD differ from those obtained from XAFS, because the former are sensitive to the lattice while the latter are local bond lengths around the X-ray-absorbing atoms. Smaller Fe atoms give shorter Fe−Pd distances, and, on average, the lattice constant is smaller. Because the radius of iron (1.27 Å) is less than that of palladium (1.38 Å), as presented in the inset in Figure 1, the Pd−Pd bond distance varies over a range of 0.274−0.276 nm (with a mismatch from 0.18% to 0.74%) as the iron content increases.

Figure 5 displays the Fourier transforms of the Fe K-edge spectra. In the case of iron foil, peaks centered at 0.220, 0.368, and 0.452 nm reveal the body-centered cubic (bcc) structure. However, the PdCFe/C electrocatalysts, unlike the iron foil, have no bcc character. The main peaks from the PdCFe/C electrocatalysts in the Fourier transform of the Fe spectra were observed at ca. 2.6 Å, which indicated the formation of an alloy structure in the electrocatalysts (see Figure 5a). Interestingly, small peaks centered at 1.5 Å exist in PdCFe/C electrocatalysts (see Figure 5b). Changing the power of k-weighting yields information on the coordination of atoms, because the k^3-weighting is sensitive to the presence of heavier atoms, whereas the k^1-weighting is sensitive to the lighter atoms. Figure 5b displays Fourier transforms of k^1-weighted EXAFS oscillations. The peaks at 1.5 Å from PdCFe/C were stronger, indicating the presence of light atoms in the first shell.

Figure 6 presents the Fe K-edge fitting results. The normalized k^3-weighted EXAFS spectra, $k^3x(k)$, were Fourier-transformed in the k-range of 3.0−11.85 Å^{-1}, to obtain the contribution of each bond pair to the Fourier transform (FT) peak. The experimental Fourier-filtered spectra were obtained by performing an inverse Fourier transformation using a Hanning window function with $r = 1-3$ Å. The S_0^2 value was fixed at 0.88, to determine the structural parameters against each bond pair.

As stated previously, the shoulders of the FT-EXAFS spectra are associated with the light atoms that were included in the Fe−Fe, Fe−C, and the Fe−Pd fitting. Table 1 summarizes the results of fitting. The contributions to the shoulders were identified. The number of degrees of freedom (N_f) is given by the following equation, where Δk represents the useful k-range of the data and Δr is the R-range of the data to be modeled.

$$N_f = \frac{2\Delta k \Delta r}{\pi} + 2 \approx 13.5$$

The fitting parameter (N_p) is 12. Therefore, $N_f > N_p$ and the analysis satisfies the minimal requirements of the IXS standard. Look again at Table 1. Three independent analyses of three samples were performed, and the fitting results were identical. Therefore, the fitting results were not an artifact of falling into the local minimum and were likely to be real. The Fe−C and Fe−Fe bond distances of the Fe_3C and Fe metal were reasonable. Table 2 presents the EXAFS fitting results for the Pd K-edge. Two shells were identified: Pd−Pd and Pd−Fe. For a bimetallic system, the following conditions must be satisfied:

$$r_{Pd-Fe} \approx r_{Fe-Pd}$$

$$N_{Pd-Fe}C_{Pd} \approx N_{Fe-Pd}C_{Fe}$$

Under these conditions, the relation "nearly equal" is used, meaning that the fitted values must agree within the limit of error.[22] As presented in Table 1, the three-shell fit for Fe−Pd, Fe−Fe, and Fe−C indicates that the bond distances and coordination numbers in the paths of Fe−Fe, Fe−Pd, and Fe−C in all PdCFe/C electrocatalysts are identical. Accordingly, the coordination environments

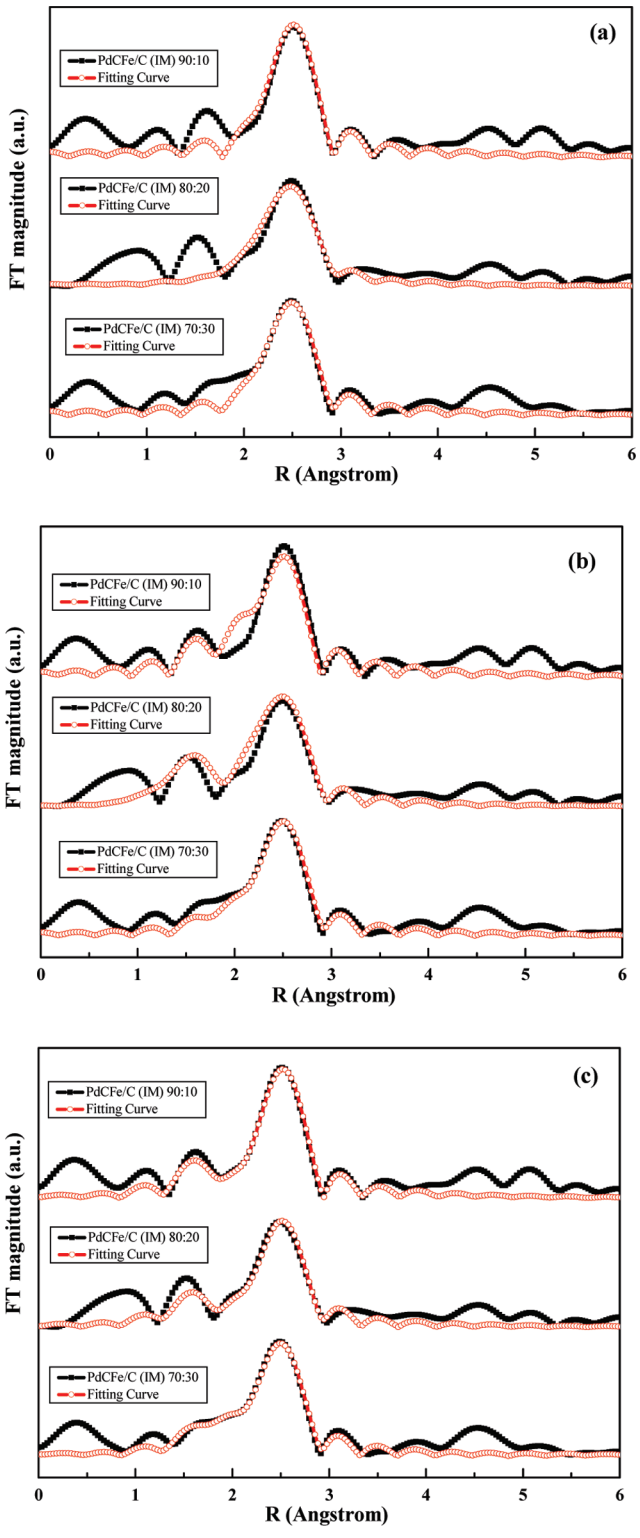

Figure 6. Fe K-edge FT-EXAFS experimental and fitted results for PdCFe/C electrocatalysts by input path of (a) Fe−Fe and Fe−Pd (b) Fe−Fe, Fe−Pd, and Fe−O, and (c) Fe−Fe, Fe−Pd, and Fe−C.

around Fe atoms can be reasonably considered to be identical. Because the Pd−Pd distance was invariable and the FePdC species and palladium metal particles coexisted in the system, it is suggested that the Fe_xC cluster was dissolved in a palladium nanoparticle.

Table 1. EXAFS Fitting Parameters at the Fe K-edge for Different PdCFe/C Samples

path	coordination number, N	bond distance, R (Å)	inner potential, ΔE_0 (eV)	Debye−Waller factor, σ^2 ($\times 10^{-3}$ Å^2)
		PdCFe/C (IM) 90:10 Sample		
Fe−Fe	1.5(7)	2.49(5)	7.4(7)	4.6(3)
Fe−Pd	5.0(8)	2.71(1)	−3.8(6)	4.4(9)
Fe−C	2.4(2)	2.08(3)	−3.4(4)	3.0(3)
		PdCFe/C (IM) 80:20 Sample		
Fe−Fe	1.3(8)	2.52(1)	8.8(1)	4.9(1)
Fe−Pd	5.2(1)	2.71(3)	−3.2(9)	6.2(4)
Fe−C	2.6(3)	2.03(5)	−8.5(3)	4.9(4)
		PdCFe/C (IM) 70:30 Sample		
Fe−Fe	1.3(1)	2.50(5)	8.3(5)	5.1(8)
Fe−Pd	5.2(9)	2.69(7)	−3.0(3)	6.0(8)
Fe−C	2.6(9)	2.12(7)	−8.6(4)	3.8(5)

Table 2. EXAFS Fitting Parameters at the Pd K-edge for Different PdCFe/C Samples

path	coordination number, N	bond distance, R (Å)	inner potential, ΔE_0 (eV)	Debye−Waller factor, σ^2 ($\times 10^{-3}$ Å^2)
		PdCFe/C (IM) 90:10 Sample		
Pd−Pd	7.3(5)	2.72(1)	5.5(6)	4.4(8)
Pd−Fe	0.6(1)	2.71(2)	−1.2(9)	3.9(7)
		PdCFe/C (IM) 80:20 Sample		
Pd−Pd	7.4(4)	2.72(6)	1.7(3)	5.3(3)
Pd−Fe	1.3(9)	2.69(8)	4.5(6)	6.5(6)
		PdCFe/C (IM) 70:30 Sample		
Pd−Pd	7.3(1)	2.72(9)	8.4(2)	5.4(8)

Other studies have noted that metallic oxides may form during the synthesis.[27−29] Travitsky et al.[30] have noted that transition-metal ions such Fe, Co, and Ni can bind on a carbon support by an anchoring effect, and that heat treatment can form Fe_xC and incorporate it into palladium nanoparticles. Therefore, we predicted the presence of iron carbide in a solid solution of PdCFe. As presented in Figure 6, a curve generated by the input paths of Fe−Pd, Fe−Fe and Fe−C fit the experimental data reasonably, indicating the incorporation of C atoms in PdCFe/C electrocatalysts and the consequent formation of a solid solution of Fe_xC and palladium.

Figure 7 depicts the proposed mechanism of formation of PdCFe/C electrocatalysts by impregnation. In this

(27) Xu, Y.; Ruban, A. V.; Mavrikakis, M. *J. Am. Chem. Soc.* **2004**, *126*, 4717.
(28) Kitchin, J. R.; Norskov, J. K.; Barteau, M. A. *J. Chem. Phys.* **2004**, *120*, 10240.
(29) Hwang, B. J.; Kumar, S. M. K.; Chen, C.-H.; Cheng, M.-Y.; Liu, D. G.; Lee, J. F. *J. Phys. Chem. C* **2007**, *111*, 15267.
(30) Travitsky, N.; Ripenbein, T.; Golodnitsky, D.; Rosenberg, Y.; Burshtein, L.; Peled, E. *J. Power Source* **2006**, *161*, 782.

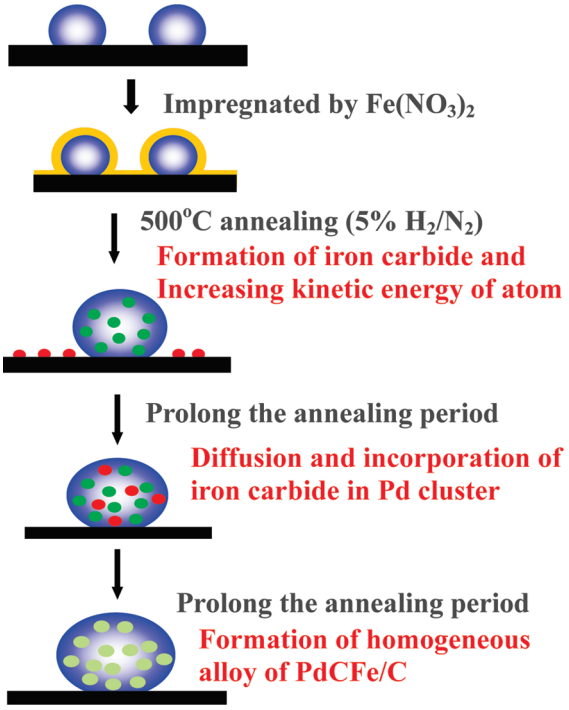

Figure 7. Proposed mechanism of formation of PdCFe/C electrocatalysts.

study, commercial Pd/C (20 wt % loading) was first impregnated with ferrous nitrate. According to Travitsky et al.,[30] Fe^{2+} ions had a tendency to be absorbed on the surface of carbon by anchoring. Since the surface area of the carbon support on Pd/C is ~100 times that of a Pd cluster, the adsorption of Fe^{2+} ions occurred mostly on the surface of the carbon support. Subsequent heat treatment in a reducing atmosphere further facilitated the reduction of Fe^{2+} ions and the formation of iron carbide species. Heat treatment facilitated the formation of carbide species, and the increase in kinetic energy caused by temperature annealing also increased the diffusion efficiency of atoms. Accordingly, we observed the migration of iron carbide species to Pd nanoclusters, becoming alloyed with the Pd lattice to form a homogeneous solid solution.

Figure 8 plots the ORR polarization curves of electrocatalysts. ORR measurements were made in 0.1 M perchloric acid that was saturated with O_2. The rate of rotation of the RDE was maintained at 1600 rpm. All of the PdCFe/C electrocatalysts were more active in ORR than Pd/C was. The half-wave potential increased as the iron content increased. The increase in ORR activity was dominated by the geometric effect[31] and the electronic effect.[32] Recent research has demonstrated that Pd_4Co is highly active toward ORR.[10,14] Wang et al.[33] elucidated the cause of the increase in activity, with reference to the Gibbs free energy of adsorption. In the ORR reaction,

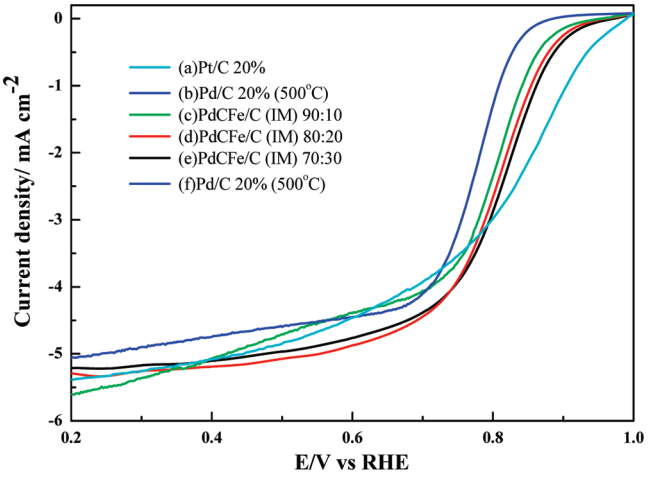

Figure 8. ORR polarization curve of Pt/C 20% (ETEK) (curve a), Pd/C 20% (500 °C) (curve b), PdCFe/C (IM) 90:10 (curve c), PdCFe/C (IM) 80:20 (curve d), and PdCFe/C (IM) 70:30 (curve e) in 0.1 M $HClO_4$ solution saturated with O_2. Sweep rate = 10 mV/s; palladium and platinum loading = 10 $\mu g/cm^2$.

oxygen first interacted with H^+ in the electrolyte to produce the −OOH species, which was subsequently adsorbed onto the surface of the electrocatalyst. According to the calculation, the Gibbs free energy of adsorption of the −OOH species at Co sites is relatively lower than that at Pd sites (i.e., oxygen molecules were captured in Co sites during the ORR reaction). After the bond with the adsorbed oxygen is cleaved, the bridge adsorption of O and OH (i.e., oxygen-containing species such as −OOH, −OH, or −O− was absorbed between the Pd and Co sites) is much more stable than the atop adsorption (i.e., oxygen-containing species directly absorbed onto the Pd and Co sites to form species such as −Pd−OH or −Co−OH) on a single Pd or Co atom, based on the calculated free energy. The subsequent transfer of electrons and addition of protons reduce the oxygen-containing species to water. In this study, the half-wave potential of ORR increased as the iron content increased. A higher iron content on the surface of the electrocatalyst may be associated with greater oxygen-adsorption capacity during the ORR. Based on the aforementioned evidence, Fe sites are believed to capture oxygen, and increasing the density of Fe sites on the surface of an electrocatalyst may reduce the Gibbs energy of oxygen adsorption in the first step of the ORR. Meanwhile, the adsorption of oxygen is not the only factor that increases the activity: the interaction between non-noble metal and palladium can also influence the geometric structure including the Pd−Pd bond distance. In 70:30 PdCFe/C (IM), the Pd−Pd bond distance is close to that obtained in the Pd_3Fe/C electrocatalyst by Shao et al.[11] Herein, investigation of the activity toward the PdCFe electrocatalyst indicates higher ORR activity, compared with Pd/C, which (result OR finding) is consistent with that of Shao et al.[11] As stated, in relation to the EXAFS fitting results, increasing the iron content increases the probability on the surface of PdCFe electrocatalyst, which increases the density of effective adsorption sites on the surface of the electrocatalyst, and thus increases activity. The lattice

(31) Wang, W.; Zheng, D.; Du, C.; Zou, Z.; Zhang, X.; Xia, B.; Yang, H.; Akins, D. L. *J. Power Source* **2007**, *167*, 243.
(32) Stamenkovic, V. R.; Mun, B. S.; Arenz, M.; Mayrhofer, K. J. J.; Lucas, C. A.; Wang, G.; Ross, P. N.; Markovic, N. M. *Nat. Mater.* **2007**, *6*, 241.
(33) Gou, Y.-G.; Hu, J.-S.; Wan, L.-J. *Adv. Mater.* **2008**, *20*, 2878.

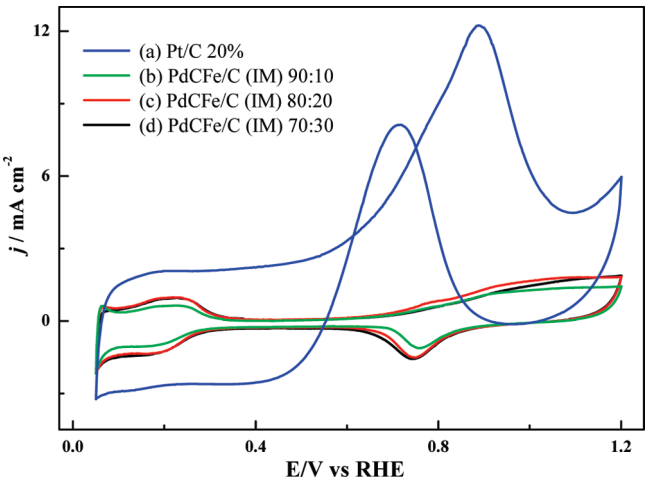

Figure 9. Cyclic voltammograms (CVs) of the GC electrode coated with Pt/C 20% (ETEK) (curve a), PdCFe/C (IM) 90:10 (curve b), PdCFe/C (IM) 80:20 (curve c), and PdCFe/C (IM) 70:30 electrocatalyst (curve d) in 0.1 M $HClO_4$ + 0.5 M CH_3OH solution, saturated by N_2. Sweep rate = 10 mV/s; palladium and platinum loading = 10 μg/cm^2.

contraction that is caused by the addition of iron may also be responsible for the increased activity. The Pd−Pd bond distance can be adjusted by alloying Pd with Fe_xC species to optimize the activity in ORR.

Platinum-based electrocatalysts are severely poisoned by CO, which is the intermediate formed in methanol electro-oxidation[31−34] in the operation of DMFCs. When platinum metal is used as an electrocatalyst, the intermediate of methanol electroxidation, CO, is adsorbed on the surface of platinum, blocking the reactive sites that are present on the surface, resulting in low catalytic efficiency. In this study, methanol crossover is simulated by performing an electrochemical test on a palladium-based electrocatalyst in a methanol-containing solution. The CV presented in Figure 9 reveals an obvious methanol oxidation signal at ~0.71 V and 0.88 V in Pt/C (from ETEK). The oxidation current is absent from the PdCFe/C electrocatalyst, revealing strong electrochemical resistance against methanol oxidation in all PdCFe/C electrocatalysts. As stated, the use of PdCFe/C as an electrocatalyst is highly desirable, because they can eliminate the negative effect of methanol crossover on cathodes in DMFCs.

(34) Park, K.-W.; Sung, Y.-E. *J. Ind. Eng. Chem.* **2006**, *12*, 165.

Conclusion

In summary, PdCFe/C electrocatalysts with a single face-centered cubic (fcc) phase and various Pd−Pd bond distances were synthesized by impregnation. Extended X-ray absorption fine structure (EXAFS) fitting results indicated the incorporation of carbon in a PdFe alloy and the formation of a homogeneous solid solution. The oxygen reduction reaction (ORR) polarization curves demonstrate that the half-wave potential is dependent on iron content. The surface adsorption site (Fe sites) is believed to increase with the iron content. This relation will be exploited in the future to facilitate the reduction of oxygen and thus enhance the activity of PdCFe electrocatalysts toward ORR. The methanol crossover test yielded strong resistance of the PdCFe/C electrocatalysts toward ORR, which, therefore, have great potential as cathode electrocatalysts in DMFCs.

Acknowledgment. The authors would like to thank the National Science Council of the Republic of China, Taiwan (Contract No. NSC 97-2113-M-002-012-MY3) and the Industrial Technology Research Institute (ITRI), Taiwan for financially supporting this research.